AGU PUBLICATIONS

JGR

Journal of Geophysical Research: Oceans

RESEARCH ARTICLE

10.1002/2015JC011582

Observations of the vertical and temporal evolution of a Natal Pulse along the Eastern Agulhas Bank

Xavier Pivan[1], Marjolaine Krug[2,3,4], and Steven Herbette[3,5,6]

[1]School of Earth and Environment, University of Western Australia, Crawley, Western Australia, Australia, [2]Ecosystem Earth Observation, Council for Scientific and Industrial Research, Cape Town, South Africa, [3]Department of Oceanography, University of Cape Town, Cape Town, South Africa, [4]Nansen-Tutu Center for Marine Environmental Research, University of Cape Town, Cape Town, South Africa, [5]Laboratoire d'Océanographie Physique et Spatiale (UBO, IRD, CNRS, Ifremer), IUEM, Plouzané, France, [6]ICEMASA, Department of Oceanography, University of Cape Town, Cape Town, South Africa

Key Points:
- Reanalysis of RAFOS float from Kapex experiment trapped into the Natal Pulse
- Analysis of Eulerian temperature, pressure, and vertical velocity field
- Vorticity and structure of the cyclonic eddy within the Natal Pulse

Correspondence to:
X. Pivan,
xavier.pivan@hotmail.fr

Citation:
Pivan, X., M. Krug, and S. Herbette (2016), Observations of the vertical and temporal evolution of a Natal Pulse along the Eastern Agulhas Bank, *J. Geophys. Res. Oceans*, *121*, 7108–7122, doi:10.1002/2015JC011582.

Received 17 DEC 2015
Accepted 2 SEP 2016
Accepted article online 8 SEP 2016
Published online 28 SEP 2016

Abstract This study reinvestigates the work of Lutjeharms et al. (2001, 2003) who documented the properties of a Natal Pulse using isopycnal Lagrangian floats. We combined Lagrangian analyses and Eulerian maps derived from objective analysis to better describe the evolution of a Natal Pulse along three density surfaces referred to as the surface (satellite-observed), shallow (isopycnal 1026.8 kg m^{-3}), and deep (isopycnal 1027.2 kg m^{-3}) layer. Our observations show that this Natal Pulse extended to a depth of 1000 m and was associated with cyclonic relative vorticity values of about 6.5–8.5 $\times$ 10^{-5} s^{-1} in the surface and shallow layer and 4 $\times$ 10^{-5} s^{-1} in the deep layer. This Natal Pulse contributed to cross-shelf exchange through the offshore advection of Eastern Agulhas Bank water near the surface, onshore advection of South Indian Central Water and/or Indian Equatorial Water in the shallow layer, and Antarctic Intermediate Water in the deep layer. Sea surface temperature maps showed that the downstream progression of the Natal Pulse along the 3000 m isobath was related to a readjustment of its rotation axis. This readjustment advected Eastern Agulhas Bank water into the Natal Pulse eddy and triggered a SST cooling of about 3°C in the cyclonic area. The importance of a warm recirculating Agulhas plume originating from the Natal Pulse was highlighted. This warm water plume extended to a depth of 700 m and was associated with onshore velocities exceeding those experienced within the Natal Pulse eddy by a factor of 2. Our observations indicate that the June/July 1998 Natal Pulse and its associated plumes enhanced cross-shelf exchanges.

1. Introduction

The Agulhas Current is the western boundary current of the South-Indian Ocean subtropical gyre. It flows southward along the eastern shores of South Africa with a mean transport estimate of 70 Sv and current velocities often in excess of 2 m s^{-1} [*Bryden et al.*, 2005; *Beal et al.*, 2015]. Once the Agulhas Current reaches the tip of South Africa, it makes an abrupt anticyclonic turn referred to as the Agulhas Retroflection, and veers back eastward into the southern Indian Ocean as the Agulhas Return Current. At the Agulhas Retroflection, warm and salty water is leaked from the Indian Ocean to the Atlantic Ocean through the shedding of large anticyclonic Agulhas Rings. The leakage of Agulhas Current water into the Atlantic is a key component of the global thermohaline circulation [*Beal et al.*, 2011]. Variability in the Mozambique Channel and south of Madagascar is transmitted into the northern Agulhas Current in the form of deep sea eddies, which can lead to the formation of large cyclonic Agulhas Current meanders [*de Ruijter et al.*, 1999, 2002; *Schouten et al.*, 2002; *Tsugawa and Hasumi*, 2010]. These meanders, referred to as Natal Pulses, are major drivers of the oceanic variability in the region [*Bryden et al.*, 2005]. They impact on the coastal and shelf circulation [*Bryden et al.*, 2005; *Krug et al.*, 2014] and are thought to play an important role in the downstream variability of the Agulhas Current and the subsequent leakage of warm and salty Agulhas Current water into the Atlantic Ocean [*Schouten et al.*, 2002; *Rouault and Penven*, 2011].

Previous studies have shown that Natal Pulses are generated through barotropic instabilities when large offshore anticyclonic eddies interact with the Agulhas Current in the vicinity of the Natal Bight region (29°S) [*de Ruijter et al.*, 1999; *Schouten et al.*, 2002; *Tsugawa and Hasumi*, 2010]. Natal Pulses occur at irregular time intervals of 50–150 days [*de Ruijter et al.*, 1999] with an average of one to two Natal Pulses per year progressing all the way to the southern Agulhas Current region [*Rouault and Penven*, 2011]. Once triggered,

Natal Pulses travel downstream with phase speeds of about 10–20 cm s^{-1} [*Van der Vaart and de Ruijter*, 2001; *Rouault and Penven*, 2011] and then slow down to about 5 cm s^{-1} after reaching the Agulhas Bank south of 34°S [*Lutjeharms and Roberts*, 1988]. The lateral extent of Natal Pulses generally increases downstream and their size can range from about 30 km near the Natal Bight to 200 km offshore of Port Elizabeth [*Rouault and Penven*, 2011]. Both in situ and satellite observations have shown that the offshore displacement of the Agulhas Current during Natal Pulse events is associated with the presence of a cold-water core with cyclonic circulation inshore of the current [*Lutjeharms*, 2006; *Leber and Beal*, 2014]. Near the continental shelf, Natal Pulses can drive upwelling with an order of magnitude of 50–100 m per day [*Bryden et al*., 2005]. Natal Pulses are associated with long residence times and strongly impact the ecology of coastal and shelf regions [*Pineda et al*., 2007]. Although their impact has not been clearly quantified, warm water plumes and filaments associated with Natal Pulses also influence cross-shelf exchange by driving warm Agulhas water intrusions onto the shelf regions [*Krug et al*., 2014; *Jackson et al*., 2012].

There have been few in situ observations of Natal Pulses and their vertical structure and downstream evolution remains poorly studied. One of the more detailed descriptions of a Natal Pulse's structure was that provided by *Lutjeharms et al*. [2001, 2003] who analyzed the motions of isopycnal Langrangian floats deployed during the Cape of Good Hope Experiment (KAPEX) [*Boebel et al*., 1998]. Using a total of 12 floats captured inside one Natal Pulse over a period of 40 days, *Lutjeharms et al*. [2001] showed that inside the region of cyclonic motion, water particles were advected along tilted isopycnal lines, with upward/downward vertical motion at the leading/trailing edge of the meander. *Lutjeharms et al*. [2003] estimated that the rotational periods for the floats were about 3 and 6 days for the 1026.8 and 1027.2 kg m^{-3} isopycnals, respectively. Despite the insight gained thanks to the analysis of the KAPEX floats, several key questions remain unanswered. Little quantitative information is currently available on the vorticity structure of Natal Pulses, their interaction with the shelf topography and the extent to which they contribute to cross-shelf exchange and mixing. In a recent study, *Leber and Beal* [2014] provided some quantitative information on the vorticity structure of a Natal Pulse, but the synoptic nature of their measurements did not allow for the study of the evolution of this Natal Pulse.

The main objectives of this study are to better understand the interaction between the cyclonic eddy embedded in the Natal Pulse, the Agulhas Current, and the topography. For this purpose, we delve further into the historical KAPEX data set of isopycnal Langrangian floats trapped inside the June/July 1998 Natal Pulse. Using objective mapping methods, we derive Eulerian fields of water temperature, pressure, and vorticity fields, which allows for a better characterization of the Natal Pulse's dynamical and thermal structure within the 1026.8 and 1027.2 kg m^{-3} neutral density layers. Improved satellite remote sensing data sets of sea surface temperature (SST) and sea surface height (SSH) are used to complement our float observations and augment the findings of *Lutjeharms et al*. [2001, 2003]. Reinvestigating the KAPEX data set using objective mapping methods improves our understanding of how these large cyclonic meanders interact with the topography, how they contribute to cross-shelf exchange, and the manner in which they may lose energy to the surrounding flow.

This paper is organized as follows. The data and methodology are presented in section 2. In section 3, satellite-derived maps of ocean circulation and water temperature are combined with data acquired along the 1026.8 and 1027.2 kg m^{-3} neutral density layers to characterize the general circulation within the June/July 1998 Natal Pulse and the dynamic of a warm recirculating plume. In section 4, we discuss how the Natal Pulse contributes to the mixing of different water masses. The vorticity structure and evolution of the Natal Pulse is presented in section 5. Our results are summarized in section 6.

2. Data and Methods

2.1. Description of the Data Sets

2.1.1. Mean Sea Level Anomalies (MSLA)

In this study, we use the gridded maps of sea level anomalies and geostrophic velocity anomalies provided in the Ssalto/Duacs MSLA-DT all sat merged product (http://www.aviso.altimetry.fr). This product consists of a merged data set of Sea Surface Height (SSH) observations from up to four satellite altimeters. It is a daily data set available with a 1/4° spatial resolution and a 10% relative error. Surface relative vorticity anomaly (RV) is diagnosed using equation (1)

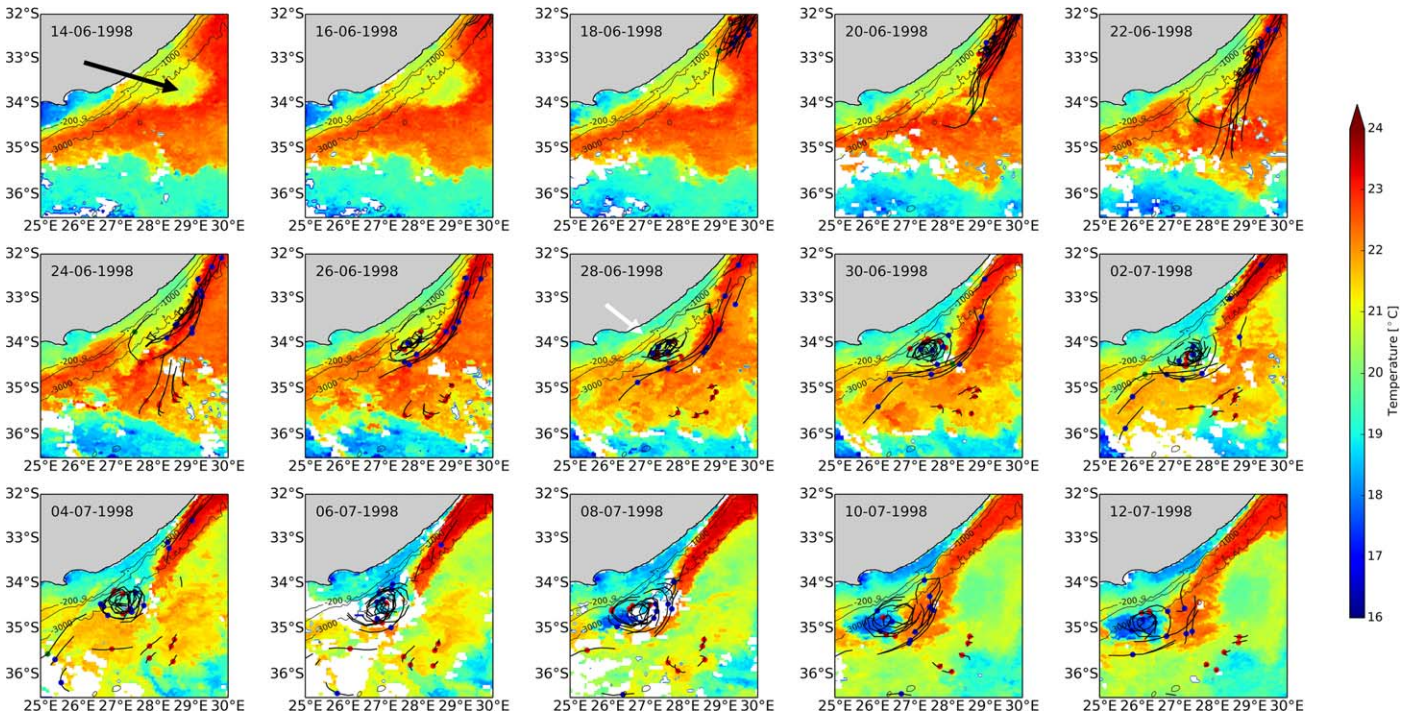

Figure 1. Southward progression of the Natal Pulse as seen in the SST imagery. Eight days SST composites are centered on the annotated date (day/month/year). Red and blue dots show the respective positions of the shallow and deep floats. A thick black line marks the path followed by the floats over a period of 4 days. The 200, 1000, and 3000 m isobaths are represented with thin black lines. The black and white arrows indicate, respectively, the Natal Pulses and the warm recirculating plume. The shallow Float 526 is a green point. GEBCO_081, with a spatial resolution of 30 arc sec grid, is used for the bathymetry in all maps.

$$RV = \partial_x v_g - \partial_y u_g, \quad (1)$$

with (u_g, v_g) the zonal and meridional geostrophic velocity component derived from altimetry.

2.1.2. Sea Surface Temperature (SST)

Pathfinder Version 5.2 (PFV5.2) sea surface temperature data are provided by the NOAA/NASA2 and the US National Oceanographic Data Center with a temporal resolution of 12 h and a spatial resolution of 4 km. The data set covers 30 years of reprocessed Advanced Very High Resolution Radiometers (AVHRR) space-based observations [*Casey et al*., 2010].

2.1.3. RAFOS Floats

RAFOS floats are acoustically tracked Lagrangian floats that drift on predetermined density surfaces (isopycnals). During the Cape of Good Hope Experiment, the so-called KAPEX program [*Boebel et al*., 2000], 47 RAFOS floats were deployed in the Agulhas Current between December 1997 and June 1998. Here we use the RAFOS float data collected between June and July 1998. The position (longitude, latitude), pressure, and temperature of the KAPEX floats were established twice daily. The KAPEX data were downloaded from the WOCE Subsurface Float Data Assembly Center (WFDAC).

2.2. Methods

The first step of our analysis was to accurately identify all floats trapped within the June/July 1998 Natal Pulse. This was done by examining the path of the RAFOS floats in conjunction with composite maps of SST, as shown in Figure 1. Natal Pulses are characterized by a region of cyclonic motion inshore of the Agulhas Current. In total, all data acquired between 15 June and 26 July was selected for our analysis of the June/July 1998 Natal Pulse. Horizontal and vertical velocities were generated from the RAFOS float data set. Time series of Lagrangian velocity was derived using the spatial displacement of the floats. The vertical velocities were derived from the pressure measured by the floats. For each RAFOS float, in order to improve our general understanding of the Natal Pulse's dynamics and evolution, time series of temperature, pressure, horizontal (u,v) and vertical (w) velocity components were plotted against each other and related to the position of the Pulse (Figures 2 and 3).

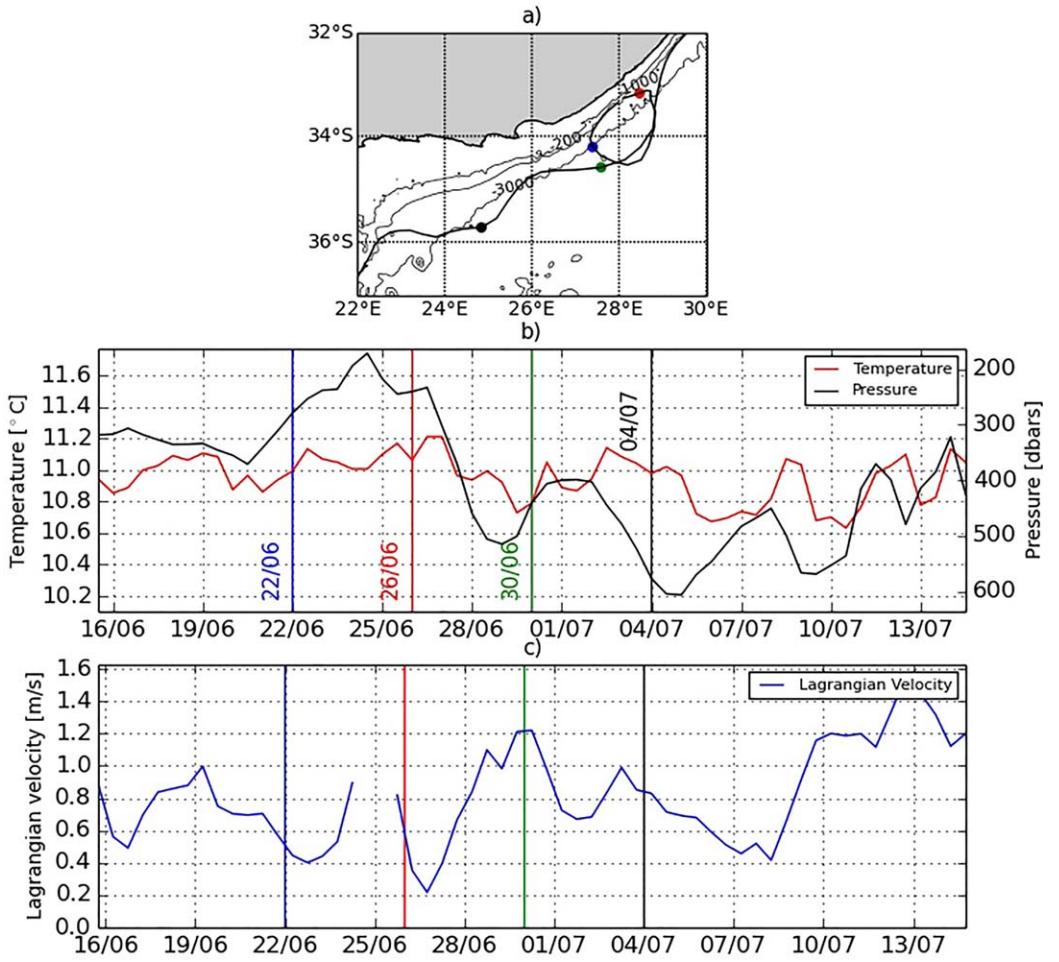

Figure 2. Shallow Float 526 features. (a) Shallow float trajectory (thick black line). The colored dots mark the float position. Each color relates to the vertical line drawn in Figures 2b and 2c. Isobath 200, 1000, and 3000 m are superimposed. (b) Time series of recorded temperature (left *y* axis) and pressure (right *y* axis). (c) Time series of Lagrangian velocity in m s^{-1}. There is missing data between 24 and 26 June.

2.2.1. Objective Analysis

After this preliminary analysis, an objective analysis was applied to the RAFOS float data set to derive gridded maps of temperature, pressure, horizontal and vertical velocity as well as relative vorticity in the 1026.8 and 1027.2 kg m^{-3} neutral density layers, from now on referred to as the shallow and deep layers [*Lutjeharms et al*., 2003]. The first cyclonic motion to coincide vertically with the cold-water core area exhibited in the SST on 23 June 1998 was used to define the start of the objective analysis period.

Objective analysis mapping is a technique that statistically determines the optimal estimate of a quantity from limited and sparse data, such as that gathered from the RAFOS floats trapped in the June/July 1998 Natal Pulse. This technique is used to produce accurate Eulerian maps of physical variables, such as temperature or wind field, from sparse irregularly sampled data, assuming a given expression of the spatial autocorrelation function. *Gandin* [1965] was the first to use objective analysis to compute Eulerian maps of pressure and wind fields in the atmosphere. Later, *Bretherton et al*. [1976] applied the technique to ocean data. Many examples of objective analysis can be found in the literature [*Arhan and Colin de Verdière*, 1985; *Chereskin and Trunnel*, 1996; *Ducet et al*., 2000]. Here we first calculated the temporal and spatial autocorrelation scales using all float data consistently trapped in the Natal Pulse between 23 June and 13 July (20 days). The Lagrangian time scale for this period was estimated to be 1.6 and 2.3 days for the shallow and deep layers, respectively. When considering all float data collected during a time interval of 2 days, an average spatial autocorrelation scale of 37 and 47 km was obtained for the shallow and deep layers,

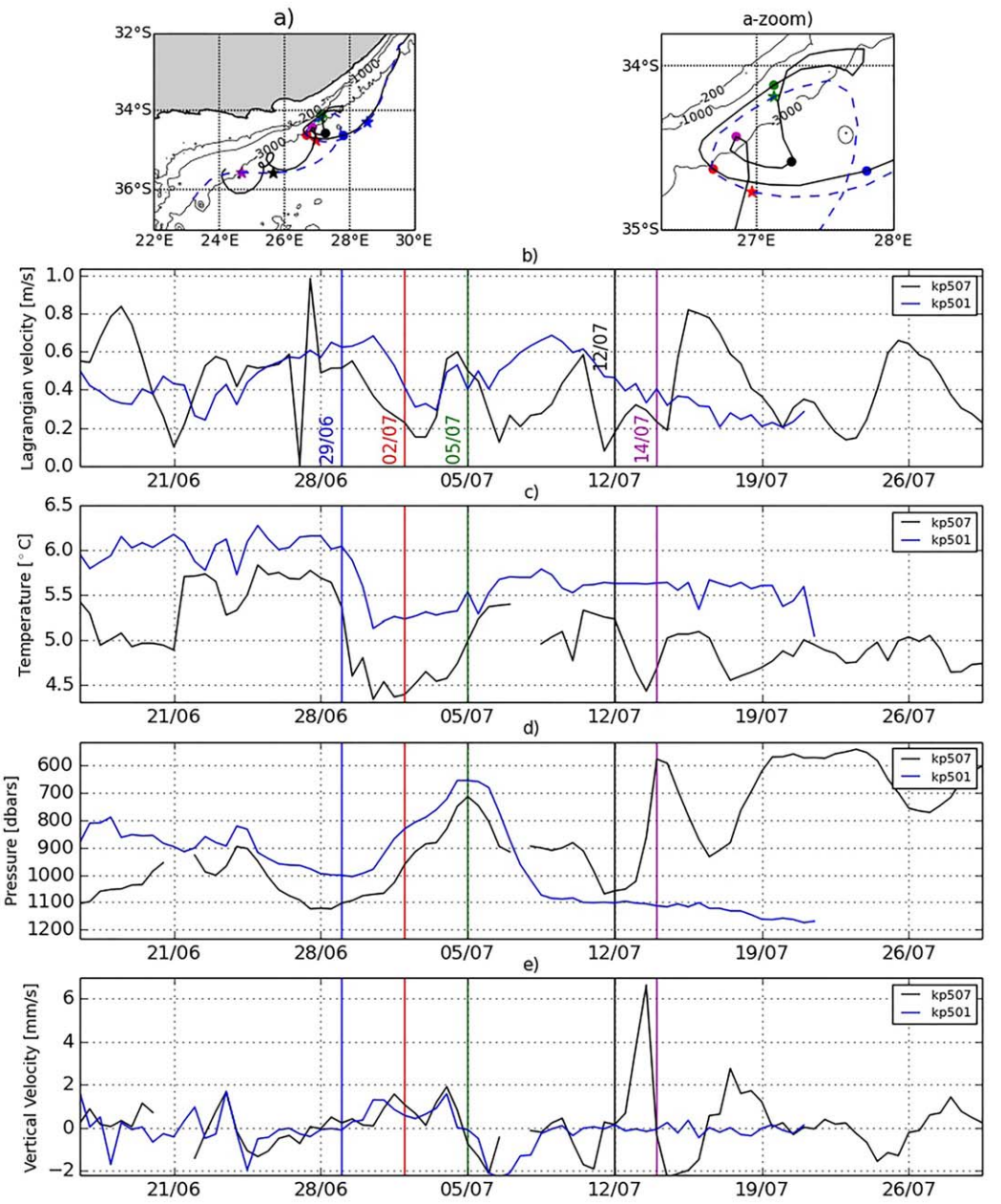

Figure 3. Deep Float 507 (thick black) and 501(thick blue) features: (a) Floats' trajectory. The colored dots and stars mark the position of Float 507 and 501, respectively. (a) Zoom of float trajectory offshore Algoa Bay. Time series of Lagrangian velocity, temperature, pressure, and vertical velocity are plotted in Figures 3b–3e, respectively.

respectively. These values were used as the typical length scale over which one collected data point may influence an estimated value. We subsequently applied the method described in *Arhan and Colin de Verdière* [1985] to generate gridded maps of estimated temperature, pressure, vertical velocity, and relative vorticity, and associated errors at time intervals of 2 days.

2.2.2. Satellite Data Set Analysis

Throughout the paper, properties of the surface layer refer to flow properties derived from satellite observations. The evolution of the surface current velocity fields was investigated using 2 day composite maps of geostrophic current anomalies. The evolution of the surface temperature was investigated through the use of 8 day composite maps of SST produced from the 12 h Pathfinder product. The satellite composites were centered on the days of the objective analysis.

3. Dynamics Derived From KAPEX Experiment

3.1. General Dynamics and Properties of the June/July 1998 Natal Pulse

The Natal Pulse studied here was spawned in the Natal Bight region (28°S) around 21 April 1998, as shown by the altimetry in *Lutjeharms et al*. [2003]. From 14 June to 12 July 1998, the Natal Pulse showed up as a region of colder water in the SST imagery (Figure 1). Floats trajectory within the cold-water region of the Natal Pulse describe cyclonic loops. The first cyclonic motions were observed on 24 June. All floats were then progressively trapped within the cyclonic core of the Natal Pulse during the following 2 days. Floats are considered to be trapped within the Natal Pulse cyclonic eddy only if they accomplish at least one cyclonic loop [*Shoosmith et al*., 2005]. In the period that followed, between 24 June and 12 July, most floats continued to describe cyclonic motions. In his analysis of the same RAFOS float data set, *Lutjeharms et al*. [2003, 2001] found a strong asymmetry between the onshore and offshore horizontal velocity: (i) for the shallow floats, onshore and offshore velocities are typically 0.4 and 0.8 m s^{-1}, respectively, and (ii) for the deep floats, onshore and offshore velocities are typically 0.35 and 0.65 cm s^{-1}, respectively. They justified the horizontal velocity asymmetry by an alongshore cyclone translation speed of about 15 cm s^{-1}. *Lutjeharms et al*. [2003] calculated vertical velocities of about 3 and 1 mm s^{-1} for the deep and shallow floats, respectively. In the next two sections, to provide a more detailed description of the thermal structure and general dynamics of the June/July 1998 Natal Pulse, we re-examine at the Lagrangian data set analyzed by *Lutjeharms et al*. [2003] and add some Eulerian analysis from our maps derived from objective analysis.

3.2. Warm Recirculating Plume

Agulhas Current meanders are often associated with warm water plumes or filaments at their leading edge [*Lutjeharms*, 2006]. These filaments and plumes drive warm (and saline) water onto the shelf, thereby contributing to cross-shelf mixing [*Swart and Largier*, 1987; *Lutjeharms et al*., 1989; *Schumann and van Heerden*, 1988]. The Natal Pulse of June/July 1998 shows up, both in the SST imagery (Figure 1) and in the temperature maps at depth (Figure 5), as a tongue of warm water that extends over the shelf, toward the northeast, in a direction opposite to the Agulhas Current (as noted by *Lutjeharms et al*. [2003]). It is located at the interface between the cyclonic core of the Natal Pulse and the coast. The warm water plume and the Agulhas Current exhibit similar high SST values (~23°C) that contrast with: (i) the SST (~20°C) encountered within the Natal Pulse's cyclonic eddy; (ii) the SST (~17°C) encountered on the Eastern Agulhas Bank, at 34°S, near Algoa Bay and St Francis Bay. At depth, several floats sampled this warm water plume. In the shallow layer, Float 526 (Figure 1, green dot) spent up to 4 days, between 22 and 24 June, trapped in the warm water plume. As it was advected toward the shelf, Figure 2 shows that it recorded the highest temperature observed in the shallow layer, with values around 11.1 ± 0.1°C, and reached some displacement velocity of 0.8 m s^{-1}, a value far in excess to the 0.4 m s^{-1} velocity recorded by all the other floats in the onshore region of the Natal Pulse. This strong velocity occurred at a pressure of 200 dbars, when the float was located near the 200 m isobath, which shows that this warm recirculating plume extended all the way down to the seabed. We believe that Float 501 and Float 507 in the deep layer also sampled the warm recirculating plume from its early stage (Figure 1). In fact, between 27 and 30 June, both floats were embedded within the Agulhas Current, when they started to initiate a cyclonic loop that brought them nearby the shelf slope. During that stage, their recorded temperature decreased from 5.7 to 4.4°C for Float 507 and from 6.1 to 5.2°C for Float 501 (Figure 3c). Then, as they progressed along the continental slope, the two floats approached each other. This convergence of the flow resulted in an increase/decrease of the recorded temperature for Float 507/501, a possible indication of diapycnal mixing. From 5 July, their trajectory started to diverge. Float 507 progressed across the continental shelf in a pressure range of 700–900 dbars and became caught in a swift north-easterly current, while Float 501 returned within the Agulhas Current. During that period, Lagrangian velocity peaked at 0.6 m s^{-1} (Float 501), and the warm water plume signature extended all the way down to 700 dbars. The Lagrangian velocities experienced by the floats when they were trapped within the plume exceeded those observed within the cyclonic core of the Natal Pulse. This disparity in flow velocities implies that water particles within the warm water plume may overshoot the region of cyclonic circulation associated with the Natal Pulse eddy to propagate upstream, thus favoring mixing and exchange across the shelf.

After a period of anticyclonic motion (from 6 to 11 July), deep Float 507 became trapped in the Natal Pulse cyclonic eddy on 12 July (black dot/line Figure 3). The period during which Float 507 became entrapped

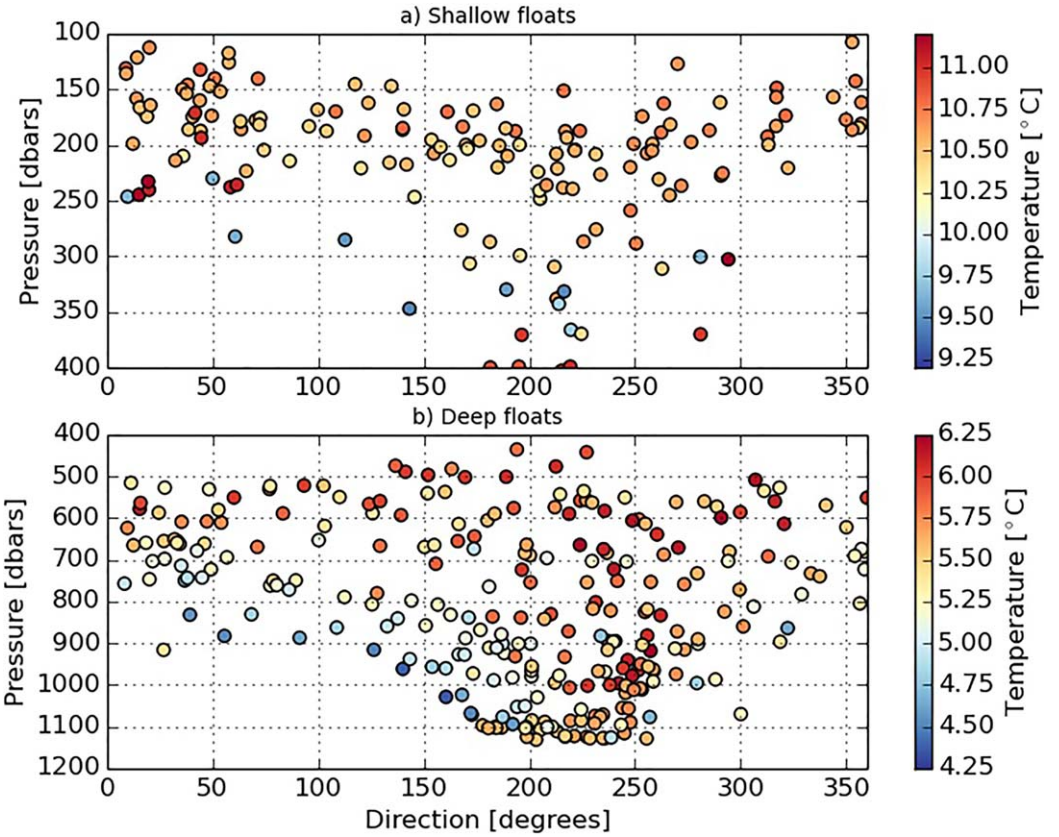

Figure 4. (a) Temperature of shallow floats (color) related to their propagating direction (degrees) and pressure (dbars). (b) Same as in Figure 4a for the deep floats. The 0, 90, 180, and 270° direction represent, respectively, east, north, west, and south.

was associated with abrupt and sudden changes in trajectory, pressure, temperature, and velocity. The Lagrangian velocity on Figure 3b (black line) decreased from 0.6 to 0.2 m s^{-1} between 10 and 14 July, then the water became strongly entrained in the Natal Pulse eddy. Pressure changes from 1050 to 600 dbars were recorded during those 2 days with a maximum vertical velocity reaching 6.3 mm s^{-1}.

The warm water plume observed in June/July 1998 acted as an agent for mixing and exchange between the region of cyclonic motions associated within the Natal Pulse eddy and the shallower shelf regions. While the warm water pulse can be considered as a separate entity to the Natal Pulse's cyclonic eddy, data collected from Float 507 showed that water exchange between the warm water plume and the Natal Pulse cyclonic eddy does occur. Data from Floats 526, 501, and 507 suggest that the June/July 1998 Natal Pulse should be viewed as a system made of several dynamically interacting subfeatures, such as a warm water plume and small anticyclonic secondary poles, all moving around a strong cyclonic eddy core. Observed velocities in the recirculating plume counter flow exceeded the Natal Pulse onshore velocity by a factor of 2.

3.3. Temperature and Associated Vertical Motions in the Natal Pulse Area

Water temperature in the shallow layer ranged from 9.3 to 11.2°C (Figure 4a). Temperatures higher than 11°C in the shallow layer were associated with the presence of a warm recirculating plume as discussed in section 3.2. Higher temperatures in the shallow layer (within a 10.3–10.9°C range) were always observed within a pressure range from 100 to 300 dbars irrespective of the flow direction. The 1026.8 kg m^{-3} neutral layer was always on its shallowest depths during periods of eastward and north-eastward flow, when floats were in the onshore arm of the cyclonic Natal Pulse eddy. During these periods, the pressure ranged from 100 to 120 dbars and water temperatures were about 10.6°C. The coldest waters on the shallow layer varied around 9.5°C and were encountered when floats were within a 250–360 dbars pressure range and are found

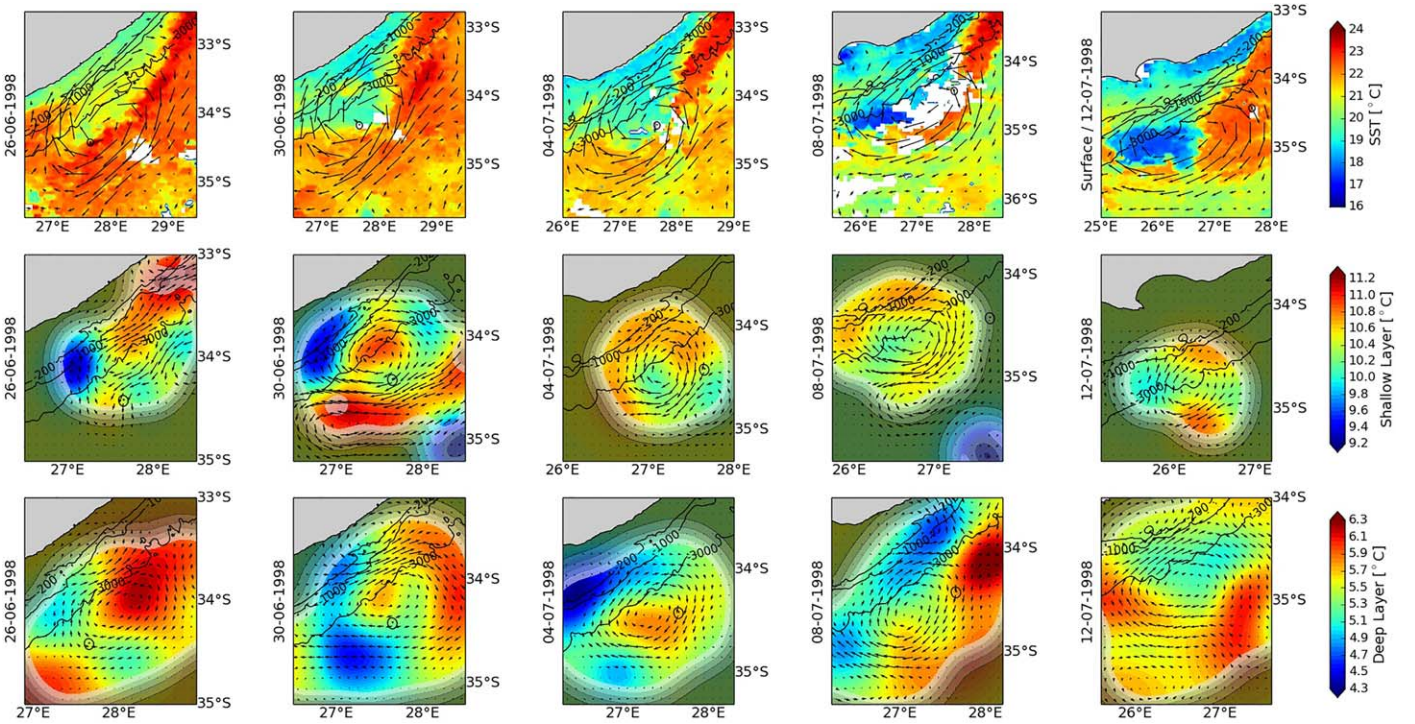

Figure 5. Objective maps of water temperature in the surface (first row), shallow (isopycnal 1026.8 kg m^{-3}, second row) and deep layer (isopycnal 1027.2 kg m^{-3}, third row) on a 1/4° × 1/4° horizontal grid at the surface, and 1/15° × 1/15 in the shallow and deep layer. Ocean current vectors are superimposed on the temperature field. In the shallow and deep layer maps, the objective analysis error field is overlaid to highlight regions where the data is reliable. All maps are centered on the Natal Pulse cyclonic eddy. The 200, 1000, and 3000 m isobaths are represented (thin black lines).

during the cyclonic counter flow with direction from 40 to 250°. Warm water of about 11°C, observed at a pressure of 400 dbars, denoted the presence of Agulhas Current water and was located in the Natal Pulse.

Within the deep layer, temperature and pressure ranged from 4.3 to 6.2°C and from 400 to 1100 dbars, respectively (Figure 4b). Pressure greater than 1000 dbars were recorded when floats were within the Agulhas Current. Our results show that the Natal Pulse eddy extended down to a depth of 1000 m, deeper than the 800 m estimated by *Lutjeharms et al*. [2003]. The vertical extend of the Natal Pulse could be observed directly from the data collected by Float 506 (not shown) while it described its second cyclonic loop within the Natal Pulse around 7 July. Similar to the shallow layer, the larger pressures were recorded when currents were flowing in a westerly/southwesterly direction (between 180 and 250° from north) while the coldest temperature which ranged from 4.3 to 5°C occurred at deeper levels of cyclonic counter flow (between 40 and 170° from north). The coldest water was recorded by Float 507 and might have been part of a recirculating Agulhas Current plume rather than trapped in the Natal Pulse eddy as discussed in section 3.2. Warmest temperature of about 6.2°C was predominantly associated with currents flowing toward the south-west, in the same direction as the mean Agulhas Current flow.

In Figure 5, the two first Eulerian maps for the shallow layer show a horizontal asymmetry in the water temperature distribution. The coldest area, with temperature of about 9.5°C, was noticed closer to the shore centered at 27°E and 34°E. To the northeast of that region near 28°E and 33.5°S, warmer waters of about 11°C were encountered and represent the warm recirculating plume mentioned in the previous section. Pressure maps (Figure 6) related to these 9.5/11°C temperature patches exhibit similar onshore/offshore variations with values of about 400/200 dbars. It does show that the two extreme temperatures observed on the shallow layer during this 20 day period occurred in a similar time and in close vicinity; thus, strong temperature and salinity gradient are found in small spatial scale on the same neutral density layer. This implies that the Agulhas recirculating plume is saltier than the cold water trapped within the cyclonic eddy. After 30 June, these cold and warm water masses are no longer represented in the shallow layer maps (Figure 5) because the float that was sampling the colder region stopped providing data and Float 526 travelled to

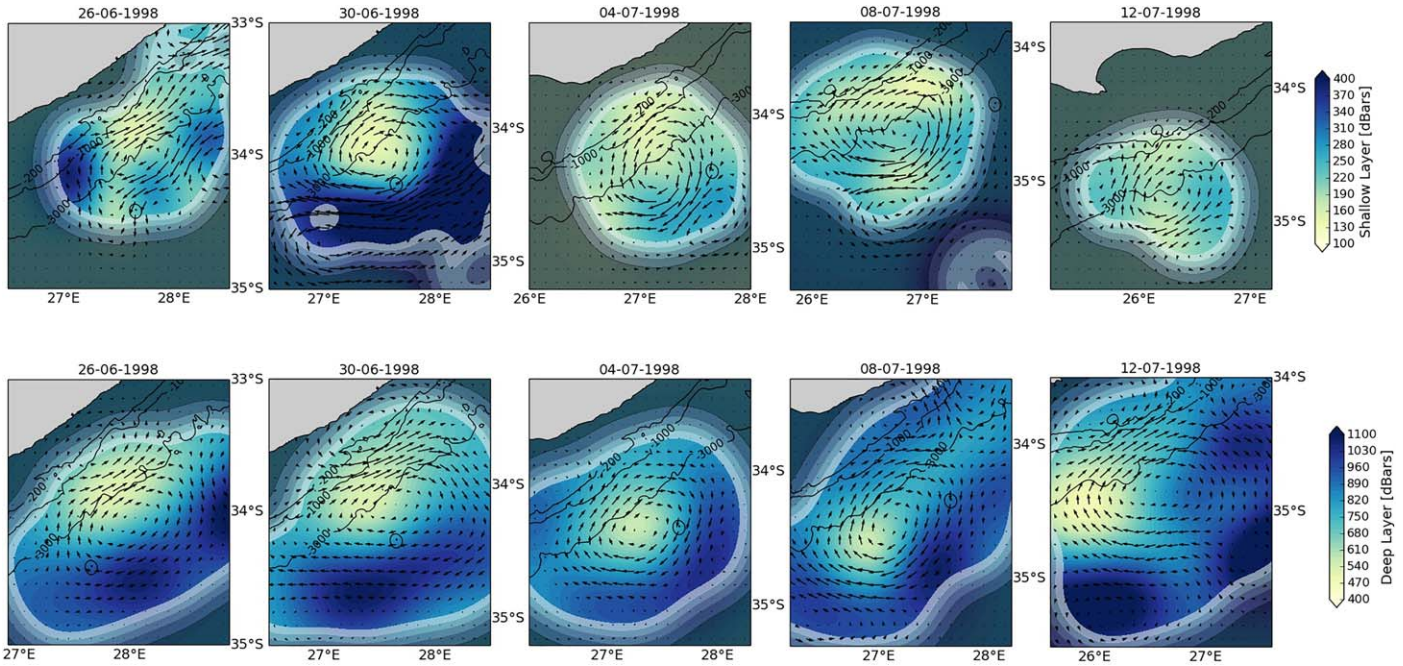

Figure 6. Objective maps of pressure fields in the shallow (isopycnal 1026.8 kg m^{-3}, first row) and deep layer (isopycnal 1027.2 kg m^{-3}, second row) on a horizontal grid of 1/15° × 1/15. Ocean current vectors are superimposed on the pressure field. In the shallow and deep layer maps, the objective analysis error field is overlaid to highlight regions where the data are reliable. All maps are centered on the Natal Pulse cyclonic eddy. The 200, 1000, and 3000 m isobaths are represented (thin black lines).

the Agulhas Current, away from the Natal Pulse area. Then, the temperature observed along the shallow layer is more homogeneous (10–10.7°C) and the pressure varies from 130 to 220 dbars in the onshore and offshore regions of the cyclone.

Along the shallow layer, the two first shallow maps in Figures 5 and 7 show a strong coherence between the horizontal temperature distribution and the vertical velocity fields. Upwelling is observed over the cold region centered at about 27°E, 34°S with upward vertical velocity ranging between 1 and 1.5 mm s^{-1}. In the warmer area, north-east of the cold region, downwelling occurs. Vertical velocities in the downwelling region have smaller values of about 0.5 mm s^{-1}. In section 3.2, we noted that the warm water plume originating from the Agulhas Current does not form part of the Natal Pulse's cyclonic eddy due to its different dynamical properties. If we disregard the vertical velocities associated with the warm water plume, we see that the strongest vertical velocities within the cyclonic core of the Natal Pulse are associated with the colder water masses and upwelling at the leading edge of the Natal Pulse. The large vertical velocities observed between the 26 and 30 June were associated with large pressure gradients along the shallow isopycnal layer, with pressure variations up to 160 dbars.

Shallow layer maps of vertical velocity in Figure 7 exhibit values such as 0.5–1 mm s^{-1} from 4 July onward. Large pressure variations along the shallow isopycnal therefore appear to drive horizontal temperature divergence within the Natal Pulse's cyclonic core. Vertical velocities along the deeper layer exhibit larger values from 1 mm s^{-1} on 30 June to 3 mm s^{-1} on 8 July. It is coherent with the larger range of pressure fluctuations observed along that isopycnal (from 400 to 1100 dbars, Figure 6). The calculated vertical velocities are consistent with those reported by *Lutjeharms et al.* [2003]. Strong temperature gradients are observed along the deep layer and throughout the period of study. The horizontal pattern of the temperature field remains similar to that observed along the shallow layer with generally colder water encountered on the inshore and leading edge of the cyclonic eddy and warmer water found offshore and in the upstream regions (Figure 5). Again, the observed vertical velocity is in general agreement with the temperature distribution with the occurrence of upwelling at the downstream edge of the Natal Pulse's cyclonic eddy and downwelling in the upstream regions. The more random nature of the float trajectories along the deep isopycnal, as shown by Float 507 and temperature map, should favor mixing. The vertical velocity in this layer appears to be less dependent of the temperature than in the shallow isopycnal.

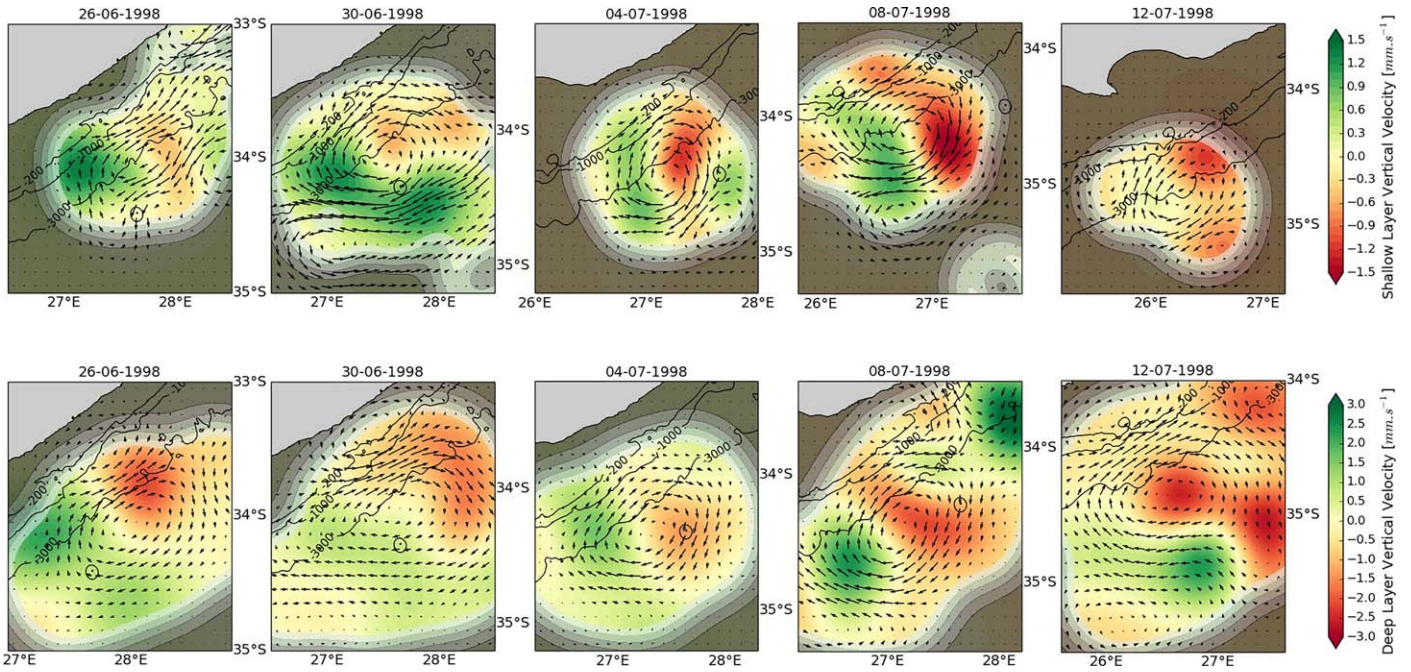

Figure 7. Objective maps of vertical velocity in the shallow (isopycnal 1026.8 kg m^{-3}, first row) and deep layer (isopycnal 1027.2 kg m^{-3}, second row) on a 1/15° × 1/15° horizontal grid. Ocean current vectors are superimposed on the vertical velocity field. The objective analysis error field is overlaid to highlight regions where the data are reliable. All maps are centered on the Natal Pulse cyclonic eddy. The 200, 1000, and 3000 m isobaths are represented (thin black lines).

4. Mixing and Water Masses Budget

4.1. Water Masses Within the Natal Pulse

Figure 8 shows a T-S diagram of temperature data collected by the isopycnal floats and salinities derived as suggested by *Boebel et al*. [1995]. Corresponding salinity values were in a range of 34.6–34.95 and 34.25–34.5 for the shallow and deep floats. From the classification table of the water masses in the region given by *Emery and Meincke* [1986], we identified Indian Equatorial Water (IEW) [8.0–23°C, 34.6–35.0] and South Indian Central Water (SICW) [8.0–25.0°C, 34.6–35.8] for the shallow layer and Antarctic Intermediate Water (AAIW) [2–10°C, 33.8–34.8 PSU] for the deep layer. This results differs from in situ observations collected during a transect through the Agulhas Current in February/March 2003 [*Beal et al*., 2006]. This transect showed that (i) South Indian Central Water (SICW) and Red Sea Water (RSW) masses were found at the inshore edge of the Agulhas Current in a range of neutral density from 1026.4 to 1027.0 kg m^{-3} for the SICW and from 1027.0 to 1027.92 kg m^{-3} for RSW and (ii) AAIW was predominantly found on the offshore edge of the Agulhas Core in the same neutral density range as the RSW. Nevertheless, not enough hydrographic observations of the Agulhas Current are currently available to categorically explain the presence of AAIW at the inshore edge of the Agulhas Current in the KAPEX data set. One hypothesis could be that the inshore/offshore extent of the AAIW within the Agulhas Current changes seasonally.

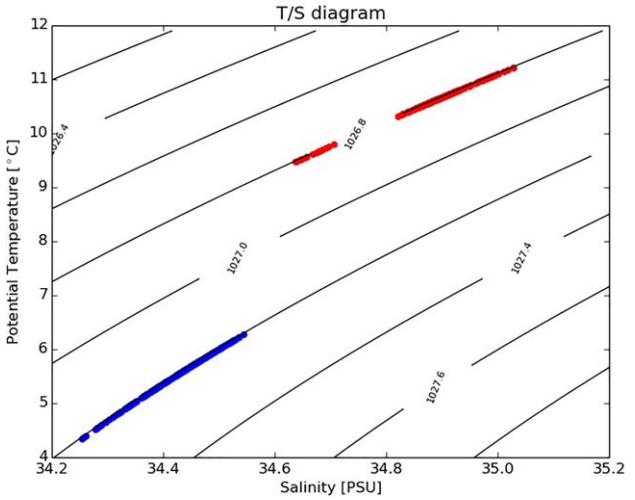

Figure 8. Temperature salinity diagram. Red and blue points represent data recorded by the shallow and deep floats, respectively. Black lines are isopycnals.

4.2. Water Mass Modifications Near Algoa Bay (34°S) Associated With the Passage of the Natal Pulse

Surface temperatures of about 19°C were observed in Algoa Bay (see 14–16 June map, Figure 1). Nevertheless, some short-term variability could also be observed during our period of interest. At the southwest corner of the bay, in between 14 and 16 June, surface temperature was as low as 17°C. It increased to 19–20°C in between 22 June and 2 July, and finally decreased again to 16–17°C. The warming of coastal waters occurred just when the warm recirculating plume entrained by the cyclonic circulation of the Natal Pulse got onto the Eastern Agulhas bank. Such warming of coastal waters has already been observed by *Goschen et al*. [2015] when a warm plume originating from the crest of an Agulhas Current meander penetrated over the shelf and moved toward the shore. The cooling episodes were most likely induced by coastal upwelling. The second cold episode coincided with the passage of the Natal Pulse and surface temperatures remained cold for 8 days. *Goschen et al*. [2015] also observed that the propagation of the Natal Pulse downstream of the Eastern Agulhas Bank could induce upwelling of cold water.

Surface temperature in the core of the Pulse itself also experienced some short-term variability. Between 24 and 26 June, the cyclone moved away from the coast as it progressed downstream along the Agulhas Bank (Figures 1 and 5). This offshore migration of the Natal Pulse was associated with a cooling of its surface inner core waters. The SST progressively decreased from 20 to 17°C. However, this decrease was not observed in the shallow and deep layers where temperature variability remained very low. Because floats within the shallow layer evolve in a pressure range of 130–220 dbars (Figure 6), this implies that the cooling only takes place at very shallow depths. This cooling could be attributed to (i) the entrainment of cold coastal water from Algoa Bay into the cyclonic core of the Natal Pulse, in a manner similar to that described by *Tsugawa and Hasumi* [2010] during the initial formation of Natal Pulses, and (ii) the upwelling of very shallow water within the Pulse. Previous observations [*Porri et al*., 2014; *Goschen et al*., 2015] have shown that coastal water from Algoa Bay is advected offshore during the passage of Natal Pulses. Our observations seem to support the first assumption. Algoa Bay and Natal Pulse waters have most likely been mixed together following the stirring of the two water masses by advective processes. Our analysis shows that this steering and mixing occurred at the region where the continental shelf widens, just south of 34°S, in between 12 and 26 July (Figures 1 and 5). There, the direction of the 3000 m isobath changes. Because the rotation axis of the cyclonic core of the Pulse tends to flow over the 3000 m isobath, this sudden change caused the Pulse to lose some vertical coherence (Figure 5). Subsequently, the Pulse went through a phase of readjustment characterized by the formation of filaments in order to regain strong vertical coherence. This phase of readjustment coincided with the observed decrease in SST within the Natal Pulse's cyclonic core. Topographic steering of the Natal Pulse may therefore be a mechanism through which coastal waters become entrained offshore and into the Natal Pulse.

5. Vorticity Modulations in the Natal Pulse's Cyclonic Core

Figure 9 shows the relative vorticity derived for the surface, shallow, and deep layers. The magnitudes of the relative vorticity (RV) were similar along the surface and the shallow layers with absolute values of about 6.5–8.5 $\times$ 10^{-5} s^{-1} but the region of cyclonic motion was larger on the surface than on the shallow layer. *Brooks and Bane* [1981] reported comparable cyclonic RV values of $+8 \times 10^{-5}$ s^{-1} at a depth of 100 m and over the 200 m isobaths in a Gulf Stream cyclonic meander. Cyclonic motion in the deep layer was less intense with maximum absolute RV of about 3–4.5 $\times$ 10^{-5} s^{-1}. Rossby numbers (Ro = Eps/f) related to the cyclonic circulation were therefore of order one, an indication that nonlinear terms associated with the centrifugal force cannot be neglected. These maximum values oscillate in phase with the elliptic (26 June, 6 July, and 10 July) or circular (30 June and 2 July) shape of the cyclonic vorticity region in the surface and shallow layer. Of course, one must be aware that the typical length scale of the cyclonic vorticity area is dependent upon the spatial autocorrelation length scale used in the objective analysis. Nevertheless, the latter was derived directly from the Lagrangian data sets.

Figure 9 shows plumes of negative RV spreading from the trailing edge of the Natal Pulse eddy. This leakage of negative cyclonic vorticity was observed both in the surface, shallow, and deep layer, throughout the 20 day period of analysis. A plume with maximum cyclonic vorticity (RV$\sim -4 \times 10^{-5}$ s^{-1}) was observed on 2 July when the Natal Pulse's cyclonic eddy had a circular shape. Within the surface and shallow layer, leakages of negative vorticity from the Natal Pulse cyclonic core may take two different forms whether the

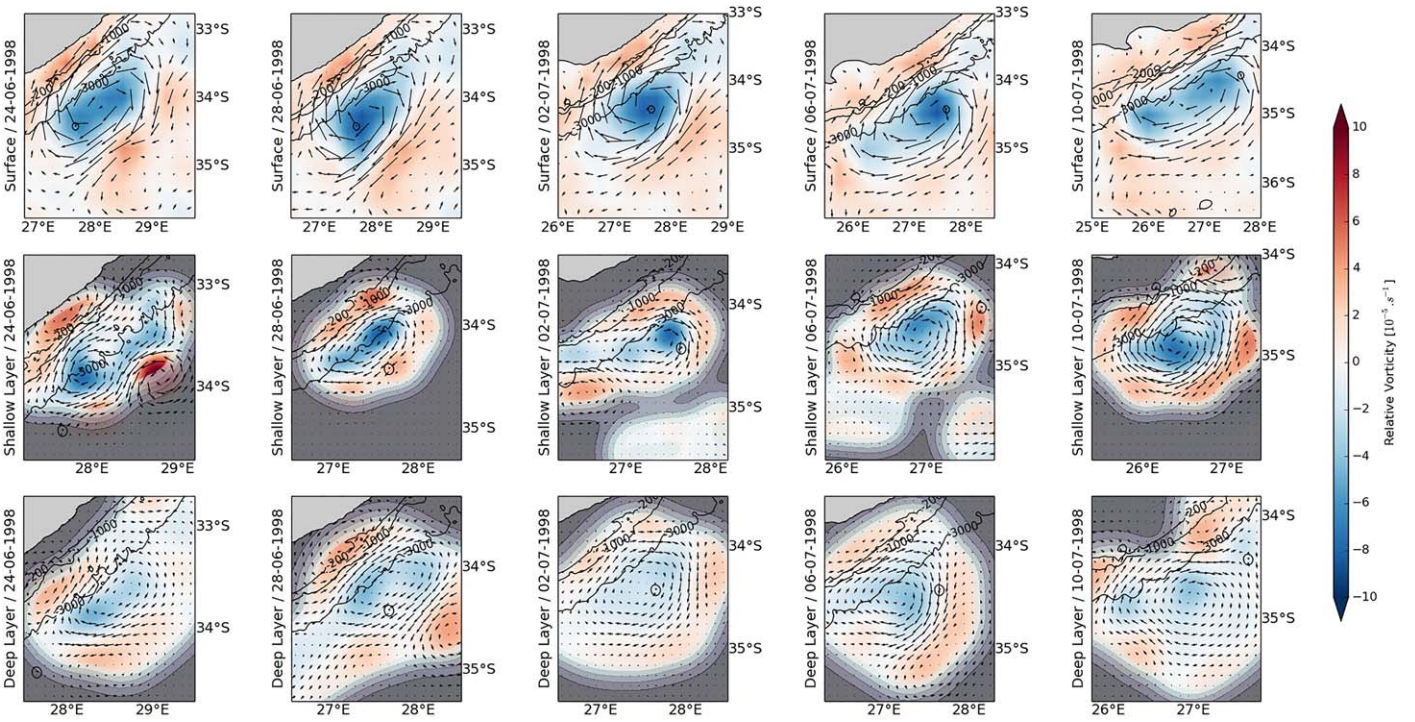

Figure 9. Objective maps of water temperature in the surface (first row), shallow (isopycnal 1026.8 kg m^{-3}, second row) and deep layer (isopycnal 1027.2 kg m^{-3}, third row) with a spatial resolution of 1/4° × 1/4° in surface and on a 1/15° × 1/15° horizontal grid in the shallow and deep layer. Ocean current vectors are superimposed on the temperature field. In the shallow and deep layer maps, the objective analysis error field is overlaid to highlight regions where the data is reliable. All maps are centered on the Natal Pulse cyclonic eddy. The 200, 1000, and 3000 m isobaths are represented (thin black lines).

cyclonic eddy is in an "open" or a "closed" phase. We define here the cyclonic eddy as "open" when there's negative vorticity spreading out of the eddy and on the contrary "closed" when negative vorticity is surrounded by positive anticyclonic vorticity. In between 24 June and 2 July, the cyclonic eddy appears to be in an "open" phase in the surface and shallow layers (Figure 9). During this phase, floats initially embedded in the Agulhas Current get trapped in the core of the Natal Pulse (Figures 1 and 9). While in an "open" phase, the core of the Pulse expelled cyclonic filaments both on its trailing (24 June) and leading edge (2 July). Between 6 and 10 July, the Natal Pulse is in a "closed" phase at least within the shallow layer. During this "closed" phase, the cyclonic core is surrounded by an annulus of anticyclonic vorticity and evolves as an isolated structure. All floats remain trapped within the cyclonic region, and leakage of cyclonic vorticity is only observed on the trailing edge of the eddy. In the deep layer, the Pulse never behaves as an isolated structure: leakage of cyclonic vorticity may occur either upstream or downstream of the region of cyclonic motion (Figure 9).

Anticyclonic vorticity patches, characterized by positive (red) RV areas in Figure 9, can be seen to surround the Pulse's cyclonic core on the three layers at any time. On 24 June, a strong anticyclone was observed in the surface (28.5°E, 35°S) and shallow layers (28.5°E, 34°S), just east of the Pulse's cyclonic core. This anticyclone could be the remains of the large Mozambique Channel anticyclonic eddy that gives birth to the June/July 1998 Natal Pulse, as it interacted with the Agulhas Current in the Natal Bight region (28°S). Nevertheless, small-scale anticyclonic regions can also be observed inshore of the Natal Pulse's cyclonic eddy, in all three layers. These secondary anticyclonic vorticity poles move around the main cyclonic core as satellites, suggesting a multipole structure for the Natal Pulse. As shown by theoretical work, their dynamical interaction with the main cyclonic core may induce some modulations in the geometry of the Natal Pulse, and be responsible for its oscillation from an elliptic to a circular shape. In Figure 10, we plotted a time series of the horizontal distance that separates the observed peaks of cyclonic vorticity in the shallow and deep layers, as well as the maximum value derived for cyclonic core. The cyclonic circulation is more intense when the maxima of cyclonic vorticity are vertically aligned, i.e., when the Natal Pulse is vertically coherent. Unfortunately, this analysis could not be extended to the surface layer due to the limitation in the spatial

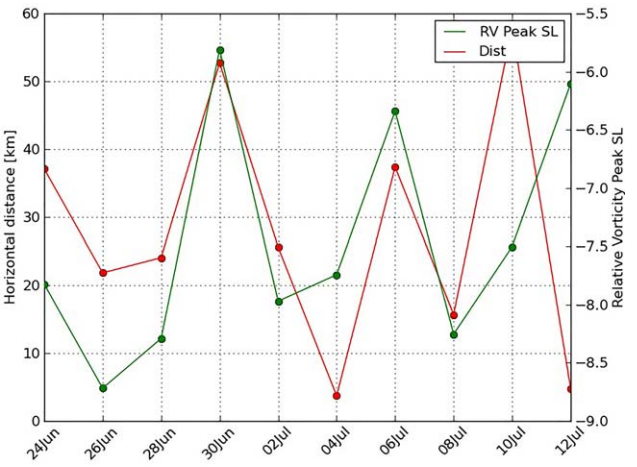

Figure 10. Distance between the minimum of relative vorticity in the shallow and deep layers (red) and peak relative vorticity [s^{-1}] in the shallow layer (green).

and temporal resolutions of the AVISO merged altimetry product. Because floats in the deep layer were not always confined within the core of the cyclonic eddy, it was not possible to establish whether the cyclonic circulation in the deep layer also intensified when the Natal Pulse was vertically coherent.

6. Discussion and Conclusion

Using maps of SST and water temperature derived along two isopycnal surfaces (1026.8 and 1027.2 kg m^{-3}), we were able to show that Natal Pulses actively contribute to the mixing of water masses between the Agulhas Current, the Natal Pulse, and the nearshore regions of the Eastern Agulhas Bank. The intrusion of warm Agulhas Current waters into the Eastern Agulhas Bank is one of the mechanisms through which this mixing may occur. *Swart and Largier* [1987] noted that these intrusions enhance the stratification above the thermocline and lead to shelf-edge upwelling of cold water below the thermocline. Our study shows that warm Agulhas Current water also penetrated onto the shelf during the KAPEX experiment in the form of a warm water plume that was spawned at the leading edge of the June/July 1998 Natal Pulse. This intrusion was accompanied with a significant increase of the Eastern Agulhas Bank SST that cancelled the cold SST signature of the Algoa Bay coastal upwelling. The intrusion of warm Agulhas Current water into the continental shelf through the formation of warm water plumes could therefore be one of the mechanisms causing the dampening of the cold SST signature reported by *Schumann et al.* [1982] during coastal upwelling favorable easterly wind events. RAFOS floats captured inside this warm water plume flowed close to the seafloor at high speed, with velocities reaching 0.8 and 0.6 m s^{-1} in the shallow and deep layer, respectively. These values were twice as high as the velocities observed on the inshore side of the Natal Pulse. The presence of strong currents near the seabed could enhance mixing on the edge of the Agulhas Bank.

Eulerian maps of temperature and vorticity, derived after performing an objective analysis on the data collected by the floats, showed the Natal Pulse remained aligned with the 3000 m isobath throughout its southward along-shelf progression. When the continental shelf break widens, south of 34°S, the Natal Pulse was topographically steered away from the coastline. This lateral offshore displacement in the Natal Pulse was associated with the offshore advection of coastal water into the cyclonic core of the Natal Pulse. This could be observed in early July 1998 when the SST inside the Natal Pulse suddenly decreased by about 3°C. Because this cooling was only observed in the SST imagery and could not be seen in the shallow and deep layers, we assumed it had to be confined to the first 100 m of the water column. The offshore advection of coastal water during the passage of a Natal Pulse could enhance a dynamically driven upwelling in the region of Port Elizabeth. This would explain the presence of cold water in that region despite the absence of upwelling favorable winds. Several studies have suggested that cold water upwelled within the Agulhas Current shear-edge eddies was then advected onshore [*Lutjeharms et al.*, 1989; *Goschen and Schumann*, 1990; *Chapman and Largier*, 1989; *Lutjeharms et al.*, 2000].

Data collected from the KAPEX RAFOS isopycnal floats confirm that water masses advected from the Agulhas Current into the Natal Pulse eddy are composed of South Indian Central Water (SICW) and/or Indian Equatorial Water (IEW) in the shallow layer and Antarctic Intermediate Water (AAIW) in the deep layer [*Emery and Meinck*, 1986]. As they propagate southward, along the eastern coast of Africa, Natal Pulses remain trapped between the inshore edge of the Agulhas Current and the east coast of South Africa. Therefore, it is likely that the predominant water masses found within Natal Pulses, when they pass the southern tip of Africa, consist of onshore Agulhas Current water and Eastern Agulhas Bank water. Our Eulerian maps

of temperature show that distinct water masses, with temperature difference as high as 2°C, are steered around by the flow in the shallow and deep layer, when the June/July 1998 Natal Pulse interacts with the shelf. According to *Beal et al*. [2006], this steering, at intermediate depth, should favor cross-frontal exchanges at the inshore edge of the Agulhas Current and mixing.

Maps of relative vorticity also show evidence of some mixing between the water masses trapped within the Natal Pulse and its surroundings. The Pulse had a strong cyclonic core characterized by negative vorticity values of -8×10^{-5} s^{-1} in the surface and shallow layer, and -4×10^{-5} s^{-1} in the deep layer. Nevertheless, we observed leakage of this cyclonic vorticity on the trailing edge of the Pulse at all depths. Such leakage induced the formation of small cyclones at the periphery of the Pulse, as observed by *Rouault and Penven* [2011]. The existence of an opposite-sign annulus around a circular vortex may give birth to barotropic instability of azimuthal mode 2, leading to the breaking of the vortex into two dipoles [*Flierl*, 1988; *Gent and McWilliams*, 1986]. The interactions between the anticyclonic satellites and the region of cyclonic motion described in section 5 might be a mechanism through which energy from the Natal Pulse's cyclonic core is leaked to the surrounding flow [*Rouault and Penven*, 2011]. *Elipot and Beal* [2015] documented the case of Agulhas Current meanders evolving as a dipole, with a cyclonic pole onshore and an anticyclonic pole offshore of the Agulhas Current. Our study suggests that Agulhas Current meanders could evolve as a multipole structure (Figure 9). Longer records would be necessary to properly identify the generation mechanism for the observed anticyclonic satellites. At this stage, it is uncertain if these anticyclonic anomalies are generated by the Natal Pulse itself or if they are caught up on the Natal Pulse's path.

Acknowledgments
We would like thanks ICEMASA and Nansen-Tutu center for their financial support for this study. We are especially grateful to Mathieu Rouault for supporting this study. The KAPEX float data set can be downloaded from ftp://ftp.whoi.edu/pub/users/woce-ssfdac/. Although we did not make use of any data from the Agulhas Current Timeseries (ACT) array, we would like to acknowledge Lisa Beal for providing some hydrographic data, even though this data were not used in this study. Krug research was funded by the CSIR Ecosystem Earth Observation group (PG EEEO023).

References

Arhan, M., and A. C. De Verdière (1985), Dynamics of eddy motions in the eastern North Atlantic, *J. Phys. Oceanogr.*, *15*(2), 153–170.
Beal, L. M., T. K. Chereskin, Y. D. Lenn, and S. Elipot (2006), The sources and mixing characteristics of the Agulhas Current, *J. Phys. Oceanogr.*, *36*(11), 2060–2074.
Beal, L. M., W. P. De Ruijter, A. Biastoch, and R. Zahn (2011), On the role of the Agulhas system in ocean circulation and climate, *Nature*, *472*(7344), 429–436.
Beal, L. M., S. Elipot, A. Houk, and G. M. Leber (2015), Capturing the transport variability of a western boundary jet: Results from the Agulhas Current Time-Series Experiment (ACT), *J. Phys. Oceanogr.*, *45*(5), 1302–1324.
Boebel, O., K. L. Shultz Tokos, and W. Zenk (1995), Calculation of salinity from neutrally buoyant RAFOS floats, *J. Atmos. Oceanic Technol.*, *12*, 923–934.
Boebel, O., et al. (1998), Float experiment studies interocean exchanges at the tip of Africa, *Eos Trans. AGU*, *79*(1), 1–8.
Boebel, O., et al. (2000), KAPEX RAFOS float data report 1997–1999; Part A: The Agulhas- and South Atlantic Current Components, p. 194, Institut für Meereskunde n der Christian-Albrechts-Universit.at-Kiel, Berichte aus dem Institut für Meereskunde 318, Kiel.
Bretherton, F. P., R. E. Davis, and C. B. Fandry (1976), A technique for objective analysis and design of oceanographic experiments applied to MODE-73, *Deep Sea Res. Oceanogr. Abstr.*, *23*(7), 559–582.
Brooks, D. A., and J. M. Bane Jr. (1981), Gulf Stream fluctuations and meanders over the Onslow Bay upper continental slope, *J. Phys. Oceanogr.*, *11*(2), 247–256.
Bryden, H. L., L. M. Beal, and L. M. Duncan (2005), Structure and transport of the Agulhas Current and its temporal variability, *J. Oceanogr.*, *61*(3), 479–492.
Chapman, P., and J. L. Largier (1989), On the origin of Agulhas Bank bottom water, *S. Afr. J. Sci.*, *85*(8), 515–519.
Chereskin, T. K., and M. Trunnell (1996), Correlation scales, objective mapping, and absolute geostrophic flow in the California Current, *J. Geophys. Res.*, *101*(C10), 22,619–22,629.
de Ruijter, W. P., P. J. van Leeuwen, and J. R. Lutjeharms (1999), Generation and evolution of Natal Pulses: Solitary meanders in the Agulhas Current, *J. Phys. Oceanogr.*, *29*(12), 3043–3055.
de Ruijter, W. P. M., H. Ridderinkhof, J. R. E. Lutjeharms, M. W. Schouten, and C. Veth (2002), Observations of the flow in the Mozambique Channel, *Geophys. Res. Lett.*, *29*(10), 1502, doi:10.1029/2001GL013714.
Ducet, N., P. Y. Le Traon, and G. Reverdin (2000), Global high-resolution mapping of ocean circulation from TOPEX/Poseidon and ERS-1 and-2, *J. Geophys. Res.*, *105*(C8), 19,477–19,498.
Emery, W. J., and J. Meincke (1986), Global water masses: Summary and review, *Oceanol. Acta*, *9*, 383–391.
Elipot, S., and L. M. Beal (2015), Characteristics, energetics, and origins of agulhas current meanders and their limited influence on ring shedding, *J. Phys. Oceanogr*, *45*(9), 2294–2314.
Flierl, G. (1988), On the instability of geostrophic vortices, *J. Fluid Mech.*, *197*, 349–388.
Gandin, L. S. (1965), Objective analysis of meteorological fields, *Q. J. R. Meteorol. Soc.*, *92*, 447.
Gent, P. R., and J. C. McWilliams (1986), The instability of barotropic circular vortices, *Geophys. Astrophys. Fluid Dyn.*, *35*(1–4), 209–233.
Goschen, W. S., and E. H. Schumann (1990), Agulhas Current variability and inshore structures off the Cape Province, South Africa, *J. Geophys. Res.*, *95*(C1), 667–678.
Goschen, W. S., T. G. Bornman, S. H. P. Deyzel, and E. H. Schumann (2015), Coastal upwelling on the far eastern Agulhas Bank associated with large meanders in the Agulhas Current, *Cont. Shelf Res.*, *101*, 34–46.
Jackson, J. M., L. Rainville, M. J. Roberts, C. D. McQuaid, and J. R. Lutjeharms (2012), Mesoscale bio-physical interactions between the Agulhas Current and the Agulhas Bank, South Africa, *Cont. Shelf Res.*, *49*, 10–24.
Krug, M., J. Tournadre, and F. Dufois (2014), Interactions between the Agulhas Current and the eastern margin of the Agulhas Bank, *Cont. Shelf Res.*, *81*, 67–79.
Leber, G. M., and L. M. Beal (2014), Evidence that Agulhas Current transport is maintained during a meander, *J. Geophys. Res.*, *119*, 3806–3817, doi:10.1002/2014JC009802.

Lutjeharms, J. (2006), *The Agulhas Current*, Springer, Berlin, Heidelberg.
Lutjeharms, J. R. E., and H. R. Roberts (1988), The Natal pulse: An extreme transient on the Agulhas Current, *J. Geophys. Res.*, *93*(C1), 631–645.
Lutjeharms, J. R. E., R. Catzel, and H. R. Valentine (1989), Eddies and other boundary, *Cont. Shelf Res.*, *9*(7), 597–616.
Lutjeharms, J. R. E., H. R. Valentine, and R. C. Van Ballegooyen (2000), The hydrography and water masses of the Natal Bight, South Africa, *Cont. Shelf Res.*, *20*(14), 1907–1939.
Lutjeharms, J. R. E., et al. (2001), Evidence that the Natal Pulse involves the Agulhas Current to its full depth, *Geophys. Res. Lett.*, *28*(18), 3449–3452.
Lutjeharms, J. R. E., O. Boebel, and H. T. Rossby (2003), Agulhas cyclones, *Deep Sea Res., Part II*, *50*(1), 13–34.
Pineda, J., J. A. Hare, and S. Sponaungle (2007), Larval transport and dispersal in the coastal ocean and consequences for population connectivity, *20*(3), 22–39.
Porri, F., J. M. Jackson, C. E. Von der Meden, N. Weidberg, and C. D. McQuaid (2014), The effect of mesoscale oceanographic features on the distribution of mussel larvae along the south coast of South Africa, *J. Mar. Syst.*, *132*, 162–173.
Rouault, M. J., and P. Penven (2011), New perspectives on Natal Pulses from satellite observations, *J. Geophys. Res.*, *116*, C07013, doi: 10.1029/2010JC006866.
Schouten, M. W., W. P. de Ruijter, and P. J. van Leeuwen (2002), Upstream control of Agulhas Ring shedding, *J. Geophys. Res.*, *107*(C8), 3109, doi:10.1029/2001JC000804.
Schumann, E. H., L. A. Perrins, and I. T. Hunter (1982), Upwelling along the South Coast of the Cape Province, South Africa, *S. Afr. J. Sci.*, *78*, 238–242.
Schumann, E. H., and I. L. van Heerden (1988), Observations of Agulhas Current frontal, *Deep Sea Res., Part A*, *35*(8), 1355–1362.
Shoosmith, D. R., P. L. Richardson, A. S. Bower, and H. T. Rossby (2005), Discrete eddies in the northern North Atlantic as observed by looping RAFOS floats. *Deep Sea Res., Part II*, *52*(3), 627–650.
Swart, V., and J. L. Largier (1987), Thermal structure of Agulhas Bank water, *S. Afr. J. Mar. Sci.*, *5*(1), 243–252.
Tsugawa, M., and H. Hasumi (2010), Generation and growth mechanism of the Natal Pulse, *J. Phys. Oceanogr.*, *40*(7), 1597–1612.
Van der Vaart, P. C. F., and W. P. M. de Ruijter (2001), Stability of western boundary currents with an application to pulse like behavior of the Agulhas Current, *J. Phys. Oceanogr.*, *31*(9), 2625–2644.